2564–2578 *Nucleic Acids Research, 2020, Vol. 48, No. 5* *Published online 29 January 2020*
doi: 10.1093/nar/gkz1188

Generation of pre-tRNAs from polycistronic operons is the essential function of RNase P in *Escherichia coli*

Bijoy K. Mohanty[1], Ankit Agrawal[2] and Sidney R. Kushner[1,2,*]

[1]Department of Genetics, University of Georgia, Athens, GA 30602, USA and [2]Department of Microbiology, University of Georgia, Athens, GA 30602, USA

Received May 16, 2019; Revised December 05, 2019; Editorial Decision December 10, 2019; Accepted January 27, 2020

ABSTRACT

Ribonuclease P (RNase P) is essential for the 5′-end maturation of tRNAs in all kingdoms of life. In *Escherichia coli*, temperature sensitive mutations in either its protein (*rnpA49*) and or RNA (*rnpB709*) subunits lead to inviability at nonpermissive temperatures. Using the *rnpA49* temperature sensitive allele, which encodes a partially defective RNase P at the permissive temperature, we show here for the first time that the processing of RNase P-dependent polycistronic tRNA operons to release pre-tRNAs is the essential function of the enzyme, since the majority of 5′-immature tRNAs can be aminoacylated unless their 5′-extensions ≥8 nt. Surprisingly, the failure of 5′-end maturation elicits increased polyadenylation of some pre-tRNAs by poly(A) polymerase I (PAP I), which exacerbates inviability. The absence of PAP I led to improved aminoacylation of 5′-immature tRNAs. Our data suggest a more dynamic role for PAP I in maintaining functional tRNA levels in the cell.

INTRODUCTION

Ribonuclease P (RNase P) is an essential riboendonuclease responsible for the 5′-end maturation of every tRNA and is found in all three domains of life (1–4). It is a ribozyme consisting of an RNA and one or more protein subunits (5,6), although protein-only variants of RNase P have recently been described (7–11). The recently identified obligatory parasitic archaeon *Nanoarchaeum equitans*, which does not have RNase P activity (4), is the single exception.

In *Escherichia coli*, RNase P is comprised of two subunits, a small protein (C5 encoded by the *rnpA* gene) and a catalytic RNA (M1 encoded by the *rnpB* gene) (12) and is essential for cell viability. In addition to its well-characterized role in 5′-end maturation of tRNAs, RNase P is required for separation of pre-tRNAs from at least seven polycistronic tRNA transcripts in *E. coli* (13–15). RNase P has also been shown to process the precursors of 4.5S RNA and tmRNA as well as several mRNAs residing in polycistronic operons (16–18).

While a mature 3′-end with a CCA trinucleotide is required for aminoacylation of a tRNA (19), there is no data to suggest that 3′-maturation of a tRNA is dependent on 5′-end maturation by RNase P. The vast majority of *E. coli* pre-tRNAs (79/86) are matured at their 3′ termini using a combination of six 3′ → 5′ exonucleases (RNase T, RNase PH, RNase D, RNase BN/Z, RNase II and polynucleotide phosphorylase) (20–22), while the rest use an one-step RNase E endonucleolytic cleavage (23). When 3′-end processing is compromised due to absence of RNase T and/or RNase PH, most tRNAs become substrates for polyadenylation by poly(A) polymerase I (PAP I, encoded by *pcnB*) (24). However, the fate of the 5′-unprocessed pre-tRNAs that are observed in the absence of RNase P is unknown.

Due to the essential nature of RNase P, temperature sensitive *E. coli* mutants in either the protein or RNA subunit have been used extensively to determine its *in vivo* activity. The commonly used *rnpA49* allele was isolated from heavily mutagenized cells (25) and was shown to contain an A to G transition resulting in a change from an arginine to histidine residue in the C5 protein (26), leading to temperature sensitive RNase P activity. In this mutant, tRNAs with unprocessed 5′-ends as well as polycistronic tRNA transcripts accumulate rapidly upon shift to the nonpermissive temperature (13–15,25).

Of the 86 tRNAs found in *E. coli*, 36 are transcribed either as monocistronic or are the first tRNA in a polycistronic transcript that have 5′ leader sequences varying from 2 to 52 nucleotides (27). In addition, pre-tRNAs resulting from RNase E cleavages of polycistronic tRNA transcripts will retain their 5′ leaders in an RNase P mutant (28–30). However, a significant number of tRNAs will be present as unprocessed polycistronic transcripts, which are processed directly at their mature 5′ termini by RNase P (13–15). Thus, RNase P is required not only to process the 5′ leader sequences on pre-tRNAs, but also to process a significant number of polycistronic tRNA transcripts.

*To whom correspondence should be addressed. Tel: +706 542 1440; Fax: +706 542 1439; Email: skushner@uga.edu
Present address: Ankit Agrawal, Clearview Healthcare Partners, Newton, MA, USA.

The exact reason why RNase P is essential *E. coli* has not been determined. It has been suggested that the 5′-unprocessed tRNAs, which occur in the *rnpA49* mutant at the nonpermissive temperature, are not aminoacylated thereby failing to support the need for increased protein synthesis at the higher temperature (31). However, several reports have demonstrated that a pre-tRNA with unprocessed nucleotides at the 5′-end can be efficiently aminoacylated at its mature 3′-end. For example, yeast aspartic tRNA with a 5′-extension has been shown to be aminoacylated *in vitro* by aspartyl-tRNA synthetase with same K_m, but with 3-fold reduction in K_{cat} values compared to the 5′-mature species (32). Furthermore, it is now known that $tRNA^{His}$ nearly universally contains an additional G residue at the −1 position at the 5′-end, which is essential for efficient aminoacylation by histidinyl-tRNA synthetase (HisRS) (33,34). In addition, complementation of a *leuU* deletion in *E. coli* with a $tRNA^{Leu}$ containing one extra nucleotide at the 5′ end (G_{-1}) (13) suggested its functionality *in vivo*.

These data are consistent with the fact that successful aminoacylation is primarily dependent on the interaction between the anti-codon loop, the CCA terminal trinucleotide and the D-stem of the tRNA with its cognate aminoacyl tRNA synthetase (35). Furthermore, complementation of an *E. coli* RNase P mutant with an RNase P derived from *Arabidopsis thaliana*, where many aberrant 5′ cleavages of tRNAs were observed (36), has indicated that 5′-maturation of tRNAs is not critical for aminoacylation and cell viability.

It has also been suggested that the essential function of RNase P is the processing an essential precursor RNA, such as 4.5S RNA encoded by *ffs* (18). However, overexpression of 4.5S RNA from a plasmid that did not require RNase P processing at its 5′-terminus to restore cell viability (15). Furthermore, recent experiments have shown that unprocessed 5′-extended 4.5S RNA supports cell viability in an *E. coli* RNase P mutant (36). It is worth noting that overexpression of the M1 RNA has been shown to partially complement the *rnpA49* mutation (37), but the exact mechanism of this partial complementation has not been yet determined.

We have previously shown that at least seven primary polycistronic tRNA transcripts are dependent on initial RNase P endonucleolytic cleavages to generate pre-tRNAs (13–15). Thus, it is expected that none of the tRNAs (at least 25) derived from these operons will be available for maturation at either end in the absence of RNase P, resulting in a significant reduction in the functional levels of these tRNAs. Accordingly, we have hypothesized that the essential function of RNase P is most likely related to the separation of pre-tRNAs from primary tRNA transcripts rather than 5′-end maturation.

In this report, we show that complementation of the *rnpA49* mutant by overexpression of M1 RNA at the permissive temperature is due to the restoration of wild type RNase P activity resulting in more efficient processing of RNase P-dependent polycistronic tRNA operons and increased availability of tRNAs for aminoacylation. We also show that a significant number of 5′-unprocessed tRNAs are substrates for aminoacylation except those with 5′-extensions ≥8 nt, which supports the hypothesis that it is not the 5′ maturation of pre-tRNAs, but the processing of RNase P-dependent polycistronic tRNA operons that is the essential function of RNase P. In addition, the polyadenylation of 5′-unprocessed pre-tRNAs by PAP I exacerbates the slow growth of an *rnpA49* mutant at both the permissive and nonpermissive temperatures by destabilizing these tRNAs. Thus, deletion of the *pcnB* gene in the *rnpA49* genetic background leads to an improved growth rate that arises from both increased steady-state levels of pre-tRNAs as well as improved aminoacylation.

MATERIALS AND METHODS

Bacterial strains and plasmids

All the strains used in this study were derived from MG1693 (*thyA715 rph-1*), which has a single base pair deletion in the *rph* gene, resulting in a frame-shift mutation and the loss of RNase PH activity (38). A wild-type control SK10153 (*thyA715*) containing a functional *rph* gene was generated by P1 transduction (24). SK2525 (*rnpA49 rbsD296*::Tn*10 rph-1*) has been previously described (30). The *rnpA49* allele encodes a temperature-sensitive RNase P enzyme and does not support cell viability at 44°C (25).

A P1 lysate grown on SK2525 (*rnpA49 rph-1*) was used to transduce SK10153 to obtain SK10521 (*rnpA49*). A P1 lysate grown on SK7988 (*ΔpcnB::kan rph-1*) (39) was used to transduce SK2525 and SK10521 to generate SK10297 (*rnpA49 ΔpcnB::kan rph-1*) and SK10522 (*rnpA49 ΔpcnB::kan*), respectively. A P1 lysate grown on SK10148 (*Δrnt::kan rph-1*) (30) was used to transduce SK2525 to generate SK10700 (*rnpA49 Δrnt::kan rph-1*).

The plasmids pAAK17 ($rnpB^+/Cm^R$) and pBMK83 ($hisR^+/Cm^R$) contain the p15A origin of DNA replication (15–20 copies/cell) and express the M1 RNA (*rnpB*) and $tRNA^{His}$,respectively, under the control of the *lacZ* promoter. Both plasmids were constructed by cloning a PCR (polymerase chain reaction) fragment containing the *lacZ* promoter, either the *rnpB* or *hisR* coding sequences followed by a Rho-independent transcription terminator [derived from *leuU* gene (14)] into the *Bam*HI/*Hin*dIII sites of pBMK11 (40). Both PCR fragments were generated by overlapping PCR. In order to avoid the RNase P requirement for 5′ maturation of $tRNA^{His}$, the *hisR* coding sequence was cloned so that it was transcribed starting at its mature 5′- end. SK10521 (*rnpA49*) was transformed with pAAK17 and pBMK83 to construct SK10521 and SK10779, respectively. No difference in the growth rate was observed in presence and absence of IPTG (data not shown) for either plasmid, suggesting leaky expression of both genes. pBMK14 (Cm^R) has been described previously (40). Plasmid pBMK14 (Cm^R) (with no *hisR*) (40) was transformed into SK10522 (*rnpA49*) to construct SK10778 and was used as the control.

Bacterial growth and RNA isolation

Bacterial strains were grown in Luria broth supplemented with thymine (50 μg/ml). When appropriate, tetracycline (20 μg/ml), kanamycin (25 μg/ml) or chloramphenicol (20 μg/ml) was added to the culture medium. Bacterial

growth was measured using a Klett–Summerson Colorimeter (No. 42 green filter). Unless mentioned otherwise, the cultures were initially grown at 30°C until they reached 50 Klett units above background and then were shifted to 44°C to inactivate RNase P. The cultures were maintained in exponential growth by periodic dilutions with pre-warmed Luria broth.

Steady-state RNA was isolated when the bacteria were either at 50 Klett units at 30°C (permissive temperature) or after 60 min at 44°C (nonpermissive temperature) following the shift. Total RNA for time-course analyses was isolated starting at 60 s (0 min) after the addition of rifampicin (500 μg/ml, dissolved in DMSO) and nalidixic acid (40 μg/ml, dissolved in water) to the bacterial culture. All RNA samples for northern analysis, poly(A) sizing assays and RT-PCR cloning were isolated using a modified RNA*snap*™ protocol and treated with DNase I as described previously (41). All RNA samples were initially quantified by measuring the OD_{260} using a Nanodrop (ND2000c) apparatus. To ensure equal loading during northern blotting, 500 ng of all RNA samples were separated in agarose mini gels and normalized to Vistra Green (Amersham Bioscience) stained 16S and 23S rRNA using a PhosphorImager (Storm 840, Amersham Bioscience).

Poly(A) sizing assay and analyses of tRNA 5′ and 3′ ends

The detailed protocol for the poly(A) sizing assay has been described previously (42,43). Briefly, total RNA was 3′-end labelled with ^{32}pCp and RNA ligase. Subsequently, the labeled RNA was digested with RNase A (which cleaves after C and U residues) and RNase T1 (cleaves after G residue) resulting in 3′-end labeled A polymers, which were separated on a 20% PAGE. RT-PCR cloning and sequencing of 5′–3′ ligated transcripts has also been described previously (42). The cDNAs for *hisR, cysT*, *leuX*, *pheU*, *pheV* were obtained as described before (14). The cDNAs of *serV* transcripts were cloned following the same procedure except the SERV-SACII primer (5′AGCCGCGG AGCGCCTTCAGCCTCTC3′) was used to reverse transcribe the *serV* tRNA. The cDNAs were amplified using the SERV-BAM 5′AAGCTGGATCCGGGGTTCGA ATCCCC3′) and SERV-SACII primers and cloned into BamHI/SacII sites of pWSK29 (44).

Analyses of *in vivo* aminoacylation of tRNAs

All the bacterial strains were initially grown to 50 Klett units above background at 30°C and subsequently shifted to 44°C for 1 h. The cultures were diluted periodically with prewarmed Luria broth at the appropriate temperature to maintain exponential growth. Five ml of each culture were removed before (30°C) and after one hour of growth at the 44°C and added to 5 ml of a cold 10% TCA solution and held on ice until all bacterial cultures had been harvested. In order to preserve tRNA aminoacylation, total RNA was isolated under acidic conditions as described previously (24). All the RNA samples were quantified using a Nanodrop (ND2000c). Half of the RNA samples were deacylated by treating with 0.5 M Tris (pH 9.0) for 30 min at 37°C. Subsequently, both untreated and Tris-treated samples (3 μg each) were separated on a 8% acid-urea gel at 4°C and transferred to a positively charged nylon membrane (Nytran® SPC, Whatman®) as described previously (24).

Northern analyses

Northern analyses were performed as described previously (41). Total RNA was separated in either 6 or 8% polyacrylamide gels (noted in the figure legends) containing 8 M urea in TBE [Tris–borate–EDTA buffer]. The Northern blots were probed using ^{32}P-end-labeled gene specific oligonucleotides (Supplementary Table S1). The same blot was probed successively with various probes for specific tRNAs. All Northern blots were scanned using a PhosphorImager (Storm 840, GE Healthcare) and quantified using ImageQuant TL (V7) software. All northern analyses were repeated at least three times. The quantification data (relative fold increase or decrease) mentioned in the text represent an average of three independent determinations.

RESULTS

The level of short poly(A) tails increased significantly in the *rnpA49* mutant

Previously, we have shown that 79/86 tRNAs in *E. coli*, which require 3′ → 5′ exonucleases for 3′-end maturation, become PAP I substrates in the absence of these exonucleases (24). In contrast, the three proline tRNAs, which are matured by an RNase E endonucleolytic cleavage at the CCA terminus, are not polyadenylated (23,24). Based on these findings, we sought to determine if failure to process the 5′-termini of pre-tRNAs might also make them susceptible to polyadenylation.

Initially, we performed a poly(A) sizing assay to compare the length and the distribution of poly(A) tails in *rnpA49* and 3′ → 5′ exonuclease mutants (Figure 1). The level of the poly(A) tails longer than 10 nts was almost identical in the wild type and *rnpA49* single mutant (lanes 3–4). Surprisingly, there was a 3 ± 1-fold increase in the amount of short poly(A) tails (≤10 nts) in the *rnpA49* mutant compared to the wild type control. In contrast, the loss of RNase PH and RNase T led to a 12 ± 2-fold increase in the amount of short poly(A) tails in the *Δrnt rph-1* double mutant (lane 1), demonstrating that inhibition of 3′-end maturation was more critical than 5′-end maturation for polyadenylation to occur. However, the level of short poly(A) tails increased almost an additional 2-fold (23 ± 4-fold) in the *Δrnt rph-1 rnpA49* triple mutant (lane 2), indicating a synergistic effect resulting from the failure of both 5′- and 3′-end maturation. The absence of all the poly(A) tails except a few of ≤6 nts in the *rnpA49 ΔpcnB* double mutant (lane 5) was consistent with PAP I being responsible for the addition of the tails observed in lane 4.

5′-Unprocessed pre-tRNAs are susceptible to polyadenylation

We have shown previously that the poly(A) tails added to 3′-unprocessed tRNAs in the absence of RNase T and RNase PH are usually short (<10 nt) (24,45). Thus, the increase in short poly(A) tails in the *rnpA49* mutants (Figure 1) indicated that 5′-immature tRNAs were likely targets

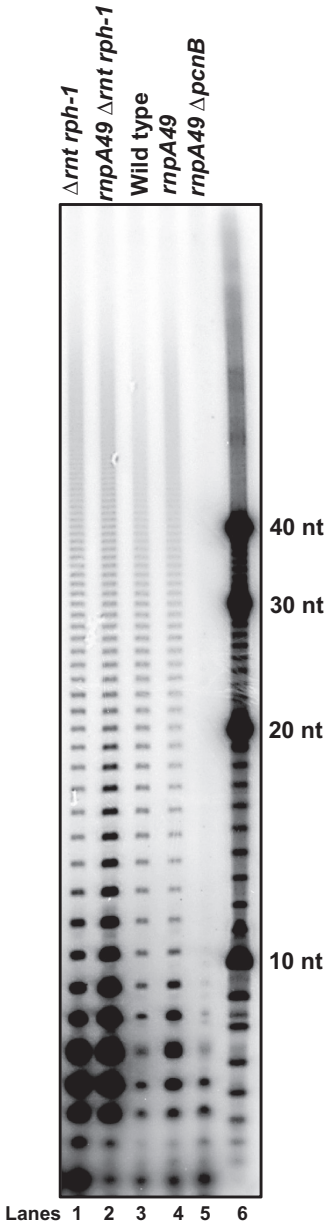

Figure 1. Distribution of poly(A) tails in various strains. Total RNA (15 μg/lane) was isolated from various strains after one hour of growth at 44°C and separated on a 20% PAGE/8 M urea after digestion with RNase A and RNase T1 as described in the Materials and Methods. The genotype of each strain is listed at the top of each lane. Lane 6, ^{32}P-labeled oligo d(A) size standards.

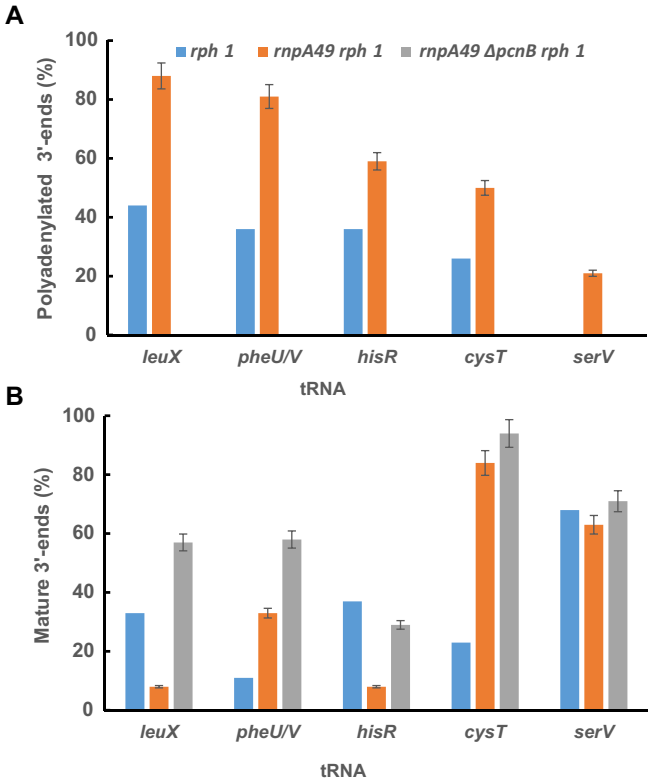

Figure 2. (**A**) Analysis of polyadenylated 3′-ends and (**B**) mature 3′-ends of tRNAs in various strains. The nucleotide sequences at the 3′ and 5′ ends of all tRNAs were identified using RT-PCR cloning of 5′–3′ self-ligated transcripts from two independent determinations as described in the Materials and Methods. Total RNA isolated from exponentially growing cultures at 44°C for 1 h after shifting from 30°C were used for self-ligation and RT-PCR. The percentages of polyadenylated 3′-ends were determined based on number of polyadenylated 3′-ends out of total number of immature 3′-ends for a particular tRNA. The percentages of mature 3′-ends were determined based on number of mature 3′-ends out of total number of sequenced 3′-ends (both mature and immature) for a particular tRNA. No polyadenylated 3′-ends was detected in the *rnpA49 ΔpcnB rph-1* mutant. The *rph-1* strain was used as control in this experiment. The identified sequences for all the tRNAs are shown in Supplementary Figure S1A–E.

for polyadenylation upon inactivation of RNase P. Accordingly, we analyzed several tRNAs isolated from the *rnpA49* mutant at the nonpermissive temperature by sequencing both their 3′- and 5′-ends as previously described (14,24,45).

tRNA^{Leu5} is processed from a monocistronic transcript encoded by *leuX*. We have previously shown that ∼19% (5/27 tRNAs) of the 5′-termini and ∼67% (18/27 tRNAs) of the 3′-termini of *leuX* tRNAs were immature in the *rph-1* strain, while ∼44% (8/18) of the 3′-immature termini contained short poly(A) tails (22) (Figure 2A). A similar analysis of the *leuX* tRNA isolated from the *rnpA49 rph-1* double mutant showed that all the tRNAs (25/25 tRNAs) had immature 5′-leader sequences, while ∼92% (23/25 tRNAs) had immature 3′-termini (Supplementary Figure S1A). More importantly, ∼88% (22/25 tRNAs) of the immature tRNAs had 1–4 untemplated A residues (Figure. 2A, Supplementary Figure S1A). The increase in the fraction of polyadenylated 5′-immature *leuX* tRNAs in the *rnpA49 rph-1* double mutant was consistent with previous results (22). However, no tRNAs with untemplated A residues beyond the three encoded A resides were observed in the *rnpA49 ΔpcnB rph-1* triple mutant (Supplementary Figure S1A), suggesting that all the tRNAs with untemplated A residues in the *rnpA49 rph-1* double mutant were generated post-transcriptionally by PAP I. The 5′-ends of all the sequenced tRNAs (23/23 tRNAs) isolated from the *rnpA49 ΔpcnB rph-1* triple mutant retained unprocessed 5′-ends. The unprocessed 5′-ends in both the double and triple mutants ranged between 7 and 13 nt (Supplementary Figure S1A) due to non-specific RNase E

cleavages within the 5′ leader region as has previously been reported (22).

Next, we analyzed the *pheU* and *pheV* tRNAs, which are transcribed as monocistronic transcripts with 5′-leader sequences of 3–4 nucleotides (46). Previously, we showed that ∼14% (4/28 tRNAs) of these species retained their 5′-leader sequences and ∼89% (25/28 tRNAs) of them had immature 3′-ends (retaining 1–3 nts trailer sequences downstream of CCA determinant) in an *rph-1* strain (46). Approximately 36% (9/25 tRNAs) of the 3′-immature termini in the *rph-1* strain contained short poly(A) tails. In the *rnpA49 rph-1* double mutant, ∼96% (23/24 tRNAs) of the *pheU* and *pheV* tRNAs retained the 5′-immature ends, while ∼67% (16/24 tRNAs) tRNAs retained the immature 3′-ends. However, the 3′-immature termini with short poly(A) tails increased to ∼81% (13/16 tRNAs) in the double mutant (Figure 2A) (46). In the *rnpA49 ΔpcnB rph-1* triple mutant, ∼92% (21/24 tRNAs) tRNAs retained their 5′-leader sequences and ∼42% (10/24 tRNAs) tRNAs had immature 3′ termini, but no immature 3′ ends had poly(A) tails (Supplementary Figure S1B).

Subsequently, we examined the *hisR* (Supplementary Figure S1C) and *cysT* (Supplementary Figure S1D) tRNAs, both of which are part of distinct polycistronic tRNA transcripts (30). RNase E endonucleolytic cleavages within the *argX hisR leuT proM* primary transcript release *hisR* pre-tRNAs with a 5′-leader of 8 nt and a 3′-trailer of 1–3 nt, while the pre-*cysT* is released with a 4 nt leader at the 5′-end and a 1–2 nt trailer at the 3′-end from the *glyW cysT leuW* primary transcript (13,14,28,30). About 25% (6/24 tRNAs) of the *hisR* pre-tRNAs retained the 8 nt 5′-leader sequence and ∼ 63% (15/24 tRNAs) had immature 3′-ends containing 1–3 encoded trailer nucleotides downstream of CCA in the *rph-1* strain. In contrast, all the 24 *his* tRNAs in the *rnpA49 rph-1* double mutant retained their 5′-leaders and 22/24 tRNAs (∼92%) had the immature 3′-termini. More importantly, the number of immature termini containing short poly(A) tails increased from 36% (4/11 tRNAs) in the *rph-1* strain to ∼59% (13/22 tRNAs) in the *rnpA49 rph-1* double mutant (Figure 2A). A similar analysis in the *rnpA49 ΔpcnB rph-1* mutant showed that ∼71% (20/28) 3′-ends retained the 1–3 nt downstream trailer sequence, but none had poly(A) tails. All 5′-ends except one were immature in the *rnpA49 ΔpcnB rph-1* triple mutant (Supplementary Figure S1C).

While all of the cloned *cysT* tRNAs were mature at their 5′-end in the *rph-1* strain, almost all of the *cysT* tRNAs retained their 5′ leader sequences in the *rnpA49 rph-1* double (98%, 49/50 tRNAs) and the *rnpA49 ΔpcnB rph-1* triple (35/35 tRNAs) mutants (Supplementary Figure S1D). Surprisingly, the number of immature 3′ termini was the highest in the *rph-1* strain (∼77%, 27/35 tRNAs) compared to the *rnpA49 rph-1* double (∼16%, 8/50 tRNAs) and *rnpA49 ΔpcnB rph-1* triple (∼6%, 2/35 tRNAs) mutants. However, the tRNAs with immature 3′-ends with short poly(A) tails was higher in the *rnpA49 rph-1* double mutant (∼50%, 4/8 tRNAs) compared to the *rph-1* strain (∼26%, 7/27 tRNAs) (Figure 2A, Supplementary Figure S1D). None of the immature 3′-ends in the *rnpA49 ΔpcnB rph-1* triple mutant were polyadenylated.

We also analyzed $tRNA^{serV}$, encoded by *serV*, which was predicted to have the longest (52 nt) 5′-leader sequence of all the *E. coli* tRNAs (27). Surprisingly, sequencing analysis showed 5′-leader sequences ranging from 3–56 nt in all genetic backgrounds (Supplementary Figure S1E), suggesting it can have a 5′-leader sequence of up to 56 nts. The multiple cleavages upstream of the mature 5′ terminus in the *rnpA49* mutants were most likely due to nonspecific endonucleolytic cleavages by RNase E as we have shown previously for the *leuX* tRNA (22). As expected, tRNAs in both the *rnpA49 rph-1* double mutant (17/27 tRNAs) and the *rnpA49 ΔpcnB rph-1* triple mutant (14/24 tRNAs) retained a higher percentage of the 5′-leader sequences ranging from ∼58–63% compared to ∼20% (4/20 tRNAs) in the *rph-1* strain. The processing of the 3′-ends was also similar in both *rnpA49* mutants except ∼25% (3/12 tRNAs) of the immature tRNAs in the *rnpA49 rph-1* double mutant had short poly(A) tails (Figures. 2A, Supplementary Figure S1E). Although no poly(A) tails were expected in the *rnpA49 ΔpcnB rph-1* triple mutant, the inability to detect any poly(A) tails in the *rph-1* strain (Supplementary Figure S1E) was unexpected. It is possible that either *serV* is not a preferred PAP I substrate or it undergoes faster 3′-end maturation thereby preventing polyadenylation.

Taken together, these data suggested that pre-tRNAs are more susceptible to polyadenylation by PAP I in the *rnpA49* mutant (Figure 2A) in agreement with the poly(A) sizing analyses (Figure 1). Furthermore, the number of tRNAs with mature 3′-ends increased in the *rnpA49 ΔpcnB rph-1* triple mutant compared to *rnpA49 rph-1* double mutant for all the tRNAs studied (Figure 2B), although no improvement in their 5′ end maturation was observed. The fraction of *leuX* tRNAs with mature 3′-ends increased from 8% (2/25 tRNAs) in the *rnpA49 rph-1* mutant to 57% (13/23 tRNAs) in the *rnpA49 ΔpcnB rph-1* triple mutant (Supplementary Figure S1A). The number of *pheU* and *pheV* tRNA mature 3′-ends increased from 33% (8/24 tRNAs) in the *rnpA49 rph-1* mutant to 58% (14/24 tRNAs) in the *rnpA49 ΔpcnB rph-1* triple mutant (Figure 2B; (46)]. The number of *hisR* tRNAs with mature 3′-ends increased from 8% (2/24 tRNAs) in the *rnpA49 rph-1* mutant to 29% (8/28 tRNAs) in the *rnpA49 ΔpcnB rph-1* triple mutant (Supplementary Figure S1C), while the number of *cysT* tRNAs with mature 3′-ends increased from 84% (42/50 tRNAs) in the *rnpA49 rph-1* mutant to 94% (33/35 tRNAs) in the *rnpA49 ΔpcnB rph-1* triple mutant (Supplementary Figure S1D). The number of *serV* tRNAs with mature 3′-ends increased from 63% (15/24 tRNAs) in the *rnpA49 rph-1* mutant to 71% (17/24 tRNAs) in the *rnpA49 ΔpcnB rph-1* triple mutant (Supplementary Figure S1E).

Suppression of the conditional lethality associated with the *rnpA49* mutant

Previous experiments have shown that the conditional lethality associated with the *rnpA49* allele could be partially reversed at 42°C by overexpressing the M1 RNA (encoded by *rnpB*) (37,47,48), although the exact mechanism of this complementation was not established. Additionally, we observed that an *rnpA49 ΔpcnB* double mutant had a faster

growth rate compared to the *rnpA49* single mutant at both permissive and nonpermissive temperatures (see below).

In a first step to determine if the improvement in growth in the presence of extra M1 RNA or the inactivation of PAP I was occurring by a similar mechanism, we cloned the *rnpB* gene into a 15–20 copy plasmid [pAAK17 (*rnpB*+/Cm^R)] and transformed it into an *rnpA49* mutant. Initially we compared the ability of RNase P mutants to grow on Luria agar plates at various temperatures (Supplementary Figure S2). As expected, all the strains grew up to a 10^{-5} dilution at 30°C. At 42°C, very weak growth of the *rnpA49* strain was observed only when undiluted. In contrast, the *rnpA49 ΔpcnB* double mutant showed some growth up to a 10-fold dilution and *rnpA49*/pAAK17 strain showed growth up to a 100-fold dilution. At 44°C, the *rnpA49* strain failed to grow, while both *rnpA49 ΔpcnB* and *rnpA49*/pAAK17 double mutants showed growth up to a 10-fold dilution.

Next, we compared the growth rate of the various *rnpA49* mutants in Luria broth (Figure 3A). The *rnpA49* single mutant grew slower at 30°C compared to the wild type control and ceased growth within 40–60 minutes after shifting to the nonpermissive temperature of 44°C. Overexpression of M1 RNA from a 15–20 copy plasmid (pAAK7/*rnpB*$^+$) in the *rnpA49* strain restored the growth rate at 30°C to the wild type level. The *rnpA49 ΔpcnB* double mutant also grew faster than the *rnpA49* single mutant, but slower than the *rnpA49*/pAAK17 strain at 30°C. Growth of both the *rnpA49 ΔpcnB* and the *rnpA49*/pAAK17 strains continued for about 60 minutes after shifting to 44°C before it significantly tapered off.

The growth phenotype of RNase P mutants shown in Figure 3A indicated that while the *rnpA49* single mutant stopped growing completely at 44°C, both the *rnpA49 ΔpcnB* and *rnpA49*/pAAK17 strains kept growing slowly at the nonpermissive temperature. Thus, we determined if cessation in cell growth at the nonpermissive temperature resulted in a loss of cell viability. Viable cell counts in all strains increased until 150 min after shifting to the nonpermissive temperature (Figure 3B). The viable cell counts from the *rnpA49* single mutant dropped significantly by 210 min and were ∼20-fold less than the wild type control. In contrast, viable cell counts in both *rnpA49 ΔpcnB* and *rnpA49*/pAAK17 strains increased during this period. However, the total number of viable cells was significantly lower in all the *rnpA49* mutants compared to the wild type control suggesting much slower cell division. Furthermore, significant differences in the growth rate and viable cell counts between *rnpA49 ΔpcnB* and *rnpA49*/pAAK17 strains (Figure 3A, B) suggested independent mechanisms of complementation in the two genetic backgrounds.

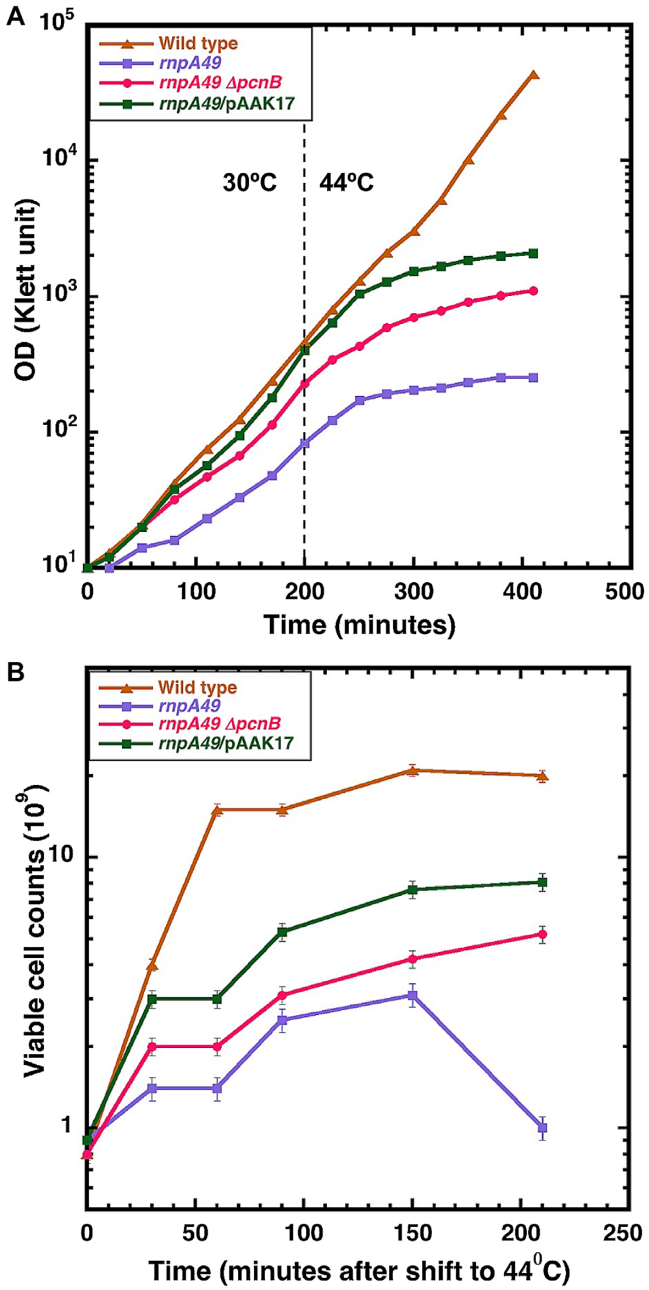

Figure 3. Comparison of growth properties of bacterial strains at different temperatures. (**A**). Growth rates of bacterial strains. All cultures were initially grown at 30°C and shifted to 44°C to inactivate RNase P when the slowest growing culture (*rnpA49*) reached Klett 50 (dash line). The faster growing cultures were diluted with pre-warmed Luria broth to maintain exponential growth. The growth of the strains measured in Klett units was plotted against time after normalization for the dilution factors. (**B**) Viable cell counts of the bacterial strains at 44°C. All the bacterial strains were grown to Klett-50 (∼0.8 × 10^9) at 30°C before shifting to 44°C (0 min). Cultures (100 μl) were removed at indicated times and viable cells were counted by dilution plating at 30°C.

Overexpression of the M1 RNA improved the processing of RNase P-dependent polycistronic tRNA transcripts at 30°C

It has been shown previously that *in vitro* the RNase P holoenzyme containing the RnpA49 protein has a lower cleavage efficiency at the permissive temperature compared to the RNase P from a wild type control (31), suggesting that its reduced activity might be responsible for the mutant's slower growth rate (Figure 3A). Consequently, the full complementation of the growth phenotype of *rnpA49* single mutant after M1 RNA overexpression at the permissive temperature (Figure 3A) indicated that the RNase P activity had been restored to wild type levels. In order to directly test this hypothesis, we analyzed the processing of *valV valW,*

leuQ leuP leuV, and *secG leuU* operons in various *rnpA49* mutants using Northern blot analysis (Figures 4, Supplementary Figures S3 and S4), since it has been shown that the initial processing of these three operons is completely dependent on RNase P (13,14).

As expected, Northern blot analysis of steady-state RNA showed no full-length *valV valW* transcripts (VW1 and VW2) at either 30°C or 44°C in the wild type control (Figure 4B). In contrast, a significant amount of unprocessed *valV valW* transcripts was observed in both the *rnpA49* single and *rnpA49 ΔpcnB* double mutants at 30°C and increased dramatically at 44°C (Figure 4B). Consequently, the mature tRNA level (M, processed fraction, PF) in these strains was lower than in the wild type control at 30°C and dropped to below 15% at 44°C. In contrast, at 30°C the VW1 and VW2 species were barely detectable in the *rnpA49*/pAAK17 strain and the mature tRNA level was similar to the wild type control. However, at 44°C the levels of the VW1, VW2 and mature tRNA (M, PF) species were at the similar levels to the *rnpA49* single mutant. Furthermore, a time-course analysis of the *valV valW* transcript (Figure 4C) showed that the VW1 and VW2 species could be detected up to 20 minutes after transcription was stopped by rifampicin addition in both the *rnpA49* single and *rnpA49 ΔpcnB* double mutants at 30°C. However, no unprocessed transcripts were observed in the wild type control and the *rnpA49*/pAAK17 strain under similar conditions. At 44°C, the unprocessed transcripts (VW1 and VW2) were detected until up to 60 minutes after rifampicin addition in all strains except the wild type control. (Figure 4C).

Northern analyses of *leuQ leuP leuV* and *secG leuU* operon transcripts showed similar results (Supplementary Figures S3 and S4). The processing of both operons was significantly inhibited in the *rnpA49* and *rnpA49 ΔpcnB* strains at the permissive (30°C) temperature. In contrast, their processing in the *rnpA49*/pAAK17 strain was normal and similar to the wild type control. Although it was expected that the processing of all three operons would be dramatically impaired at 44°C in the *rnpA49* single mutant, it was somewhat unexpected that processing did not improve in either in the *rnpA49 ΔpcnB* or *rnpA49*/pAAK17 strains at 44°C (Supplementary Figures S3 and S4).

The improvement in the growth rate of the *rnpA49 ΔpcnB* mutant was not related to changes in M1 RNA levels

Since the catalytic activity of RNase P resides in the the M1 RNA (49), partial complementation of the *rnpA49* mutation in the presence of additional M1 RNA was not entirely unexpected. In fact, overexpression of *rnpB* led to ∼5–6-fold increase in the steady-state M1 RNA level in the *rnpA49*/pAAK17 strain compared to the wild type control at both temperatures (Figure 5). However, no significant difference in the M1 RNA level was found between the *rnpA49* single and *rnpA49 ΔpcnB* double mutants (Figure 5). The lower M1 RNA levels at the nonpermissive temperature in both strains compared to the wild type control was consistent with the reported shorter half-life of the *rnpB* transcript in the *rnpA49* mutant (50).

Chargeable tRNA levels were higher in the *rnpA49 ΔpcnB* mutant

After ruling out that the changes in M1 RNA levels accounted for the improvement of the growth phenotype of *rnpA49 ΔpcnB* strain, we suspected that there was an improvement in the aminoacylation of tRNAs in the double mutant compared to the *rnpA49* single mutant based on the significant improvement in the maturation of 3′-ends of tRNAs in the *rnpA49 ΔpcnB* double mutant without any change in the 5′-end maturation (Figures 2B, Supplementary Figure S1). Previous *in vitro* and *in vivo* studies have suggested that tRNAs with unprocessed nucleotides at the their 5′-ends, but a mature 3′-end could serve as substrates for aminoacylation (13,32,36). Accordingly, several tRNAs were analyzed *in vivo* for their aminoacylation patterns in wild type, *rnpA49, rnpA49 ΔpcnB* and *rnpA49*/pAAK17 strains at permissive (P, 30°C) and nonpermissive (NP, 44°C) temperatures.

Total RNAs isolated under acidic conditions were analyzed using acid urea gel electrophoresis. In this procedure the aminoacylated tRNA runs slower prior to deaminoacylation by Tris treatment. After Tris treatment, only the aminoacylated tRNAs change mobility without any effect on the non-aminoacylated tRNAs, which may include polyadenylated as well as immature tRNAs (24). We determined the percentage of aminoacylated tRNA (PAT) in each strain as well as the relative amount of chargeable tRNA (RCT) compared to the wild type control. The PAT is calculated as the fraction of aminoacylated tRNA based on the total of the specific tRNA pool (charged and uncharged) available in that strain. The RCT is calculated as the net amount of chargeable tRNAs (those that changed in mobility after Tris treatment) in each strain compared to the wild type control.

We initially tested several tRNAs that are part of RNase P-dependent polycistronic operons. For example, $tRNA^{leu2}$ encoded by the *leuU* gene requires RNase P for its separation from the *secG leuU* polycistronic transcript (14) (Supplementary Figure S3). The percentage of *leuU* tRNA aminoacylation was similar in all genetic backgrounds at the permissive temperature [Figure 6B, PAT(P)]. At the nonpermissive temperature, the percentage of aminoacylation in the wild type and *rnpA49 ΔpcnB* strain was almost identical and was only reduced slightly in the *rnpA49* and *rnpA49*/pAAK17 strains [Figure 6B, PAT(NP)].

The amount of chargeable tRNAs remained almost identical in the wild type, *rnpA49 ΔpcnB* double mutant and *rnpA49*/pAAK17 strains at the permissive temperature [Figure 6A, lanes 5–8; 6B, RCT(P)]. However, it was already reduced in the *rnpA49* single mutant compared to the wild type control at the permissive temperature [Figure 6A, lanes 1–4, 6B, RCT(P)]. At the nonpermissive temperature, the amount of chargeable tRNA [Figure 6B, RCT(NP)] was further decreased in both the *rnpA49* single mutant (Figure 6A, lanes 11–12) and *rnpA49*/pAAK17 strains (Figure 6A, lanes 15–16). No significant reduction in the amount of chargeable tRNA in the *rnpA49 ΔpcnB* double mutant was observed (Figure 6A lane 13–14). Almost identical amounts of chargeable tRNA in the wild type control and *rnpA49 ΔpcnB* double mutant at both the permissive and non-

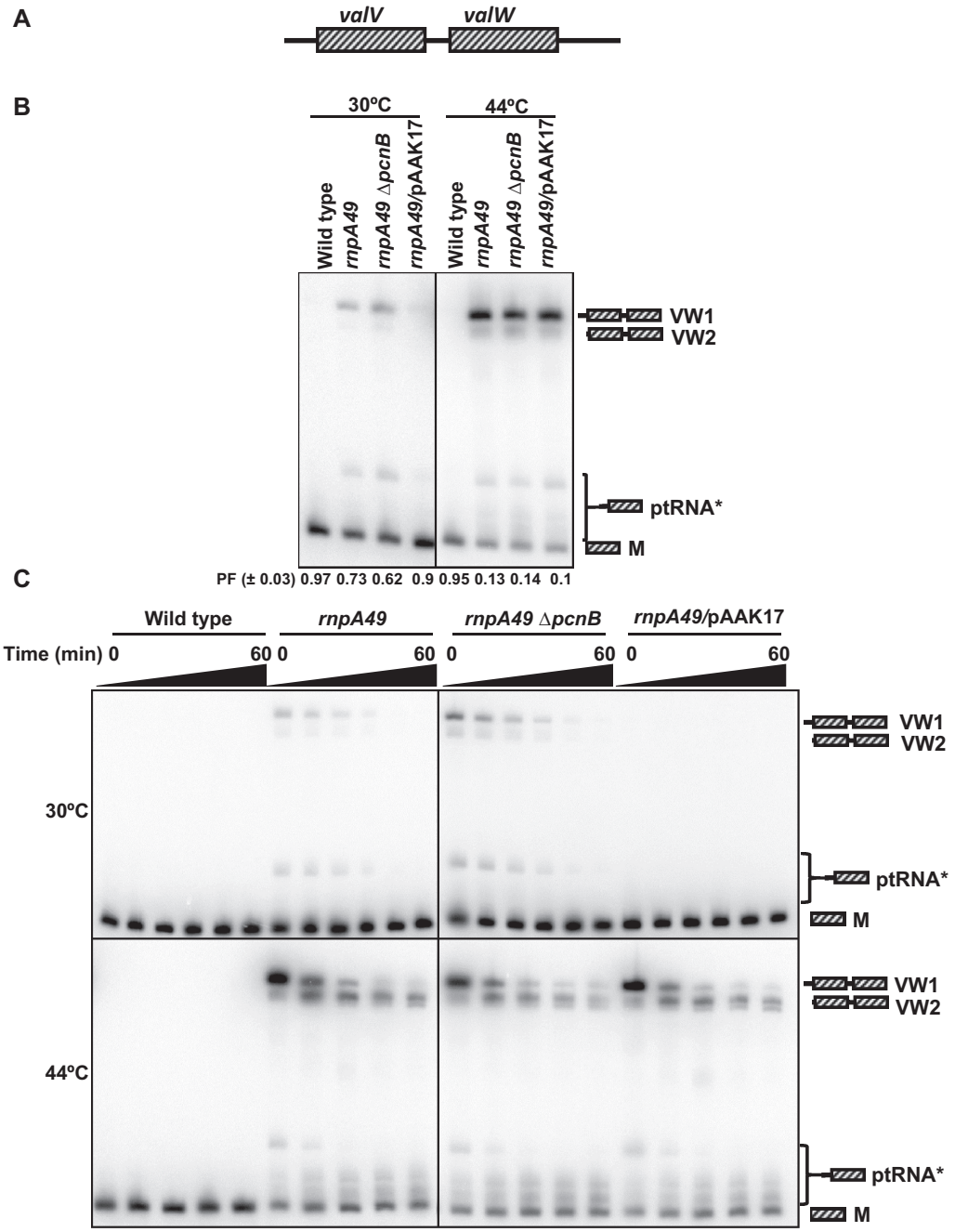

Figure 4. Analyses of *valV valW* transcripts processing in various strains by Northern blot analyses. (**A**) Graphical presentation (not drawn to scale) of *valV valW* operon in the genome. (**B**) Analysis of *valV valW* steady-state transcript level. Total RNA (10 μg/lane) isolated from exponentially growing cultures at 30°C and after one hour of growth at 44°C were used. (**C**) Comparison of *valV valW* transcript stability in various strains. Total RNA (10 μg/lane) isolated from exponentially growing culture (at 30°C and after 1 h of growth at 44°C) at various time points after addition of rifampicin and nalidixic acid were used. All RNA samples were separated on 6% PAGE with 8 M urea and transferred to nylon membrane. The blots were probed with a ^{32}P-end labeled oligonucleotide probe (VALW, Supplementary Table S1). Genotypes are shown at the top of each blot. The processing intermediates (VW1 and VW2) and mature (M) tRNA are labelled to the right of the blot (13). ptRNAs marked with (*) are due to weak hybridization to Valine tRNAs independent of *valV valW* (13). PF (processed fraction) in blot B represents the fraction of the mature tRNA (M) relative to the total amount of the tRNA (processed and unprocessed combined) in the specific strain. The numbers were calculated based on the pixel counts of each of the band in the strain and represent the average of three independent determinations. Multiple blots in each panel were run separately and merged at the vertical and/or horizontal lines.

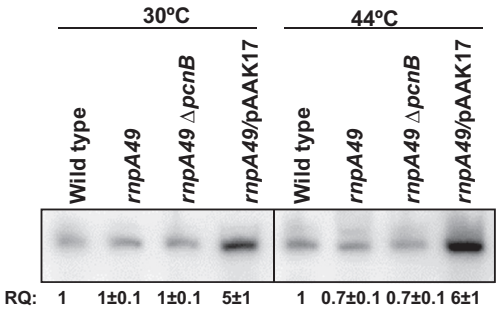

Figure 5. Determination of M1 RNA (*rnpB*) steady-state levels in various strains by Northern blot analyses. Total RNA (10 μg/lane) isolated from exponentially growing culture at 30°C and after one hour of growth at 44°C were used. All RNA samples were separated on 6% PAGE with 8 M urea and transferred to a nylon membrane. The blots were probed with a ^{32}P-end labelled oligonucleotide probe (rnpb + 393, Supplementary Table S1). Genotypes are shown at the top of each blot. The RNA samples were run on two gels to accommodate all the samples and merged at the vertical line. RQ (relative quantity) was determined by taking the pixel counts [using ImageQuant TL software (V7)] of the wild type strain as 1. The numbers represent the average of three independent determinations.

permissive temperature suggested that the 5′-unprocessed tRNAs in the double mutant were stabilized and aminoacylated in the absence of PAP I. Overexpression of *rnpB* (M1 RNA), which complemented the *rnpA49* allele at the permissive temperature, failed to do so at the nonpermissive temperature (compare Figure 6, lanes 7–8 and 15–16).

It has been shown previously that the *leuU* pre-tRNAs that accumulate in the *rnpA49* mutant contain 3′-mature termini and 5′-immature termini with 5–11 nt extensions due to non-specific RNase E cleavages downstream of *secG* mRNA (14). Multiple higher molecular weight bands in the *rnpA49* mutants at the nonpermissive temperature were consistent with the accumulation of such 5′ unprocessed pre-tRNAs (Figure 6A, lanes 11–16). Surprisingly, these bands also changed mobility and became smaller after alkaline treatment suggesting aminoacylation at the 3′ end. Similar results were also obtained for *leuT, leuP, leuQ, leuV, valV, valW, metT* and *metU* tRNAs (data not shown), which are also transcribed as part of RNase P-dependent polycistronic transcripts (13,43).

Next, we tested tRNAs that are independent of initial RNase P processing, such as *hisR, cysT, pheU* and *pheV*. While *hisR* and *cysT* are unique tRNAs and are part of RNase E-dependent polycistronic tRNA operons (30), the *pheU* and *pheV* tRNAs are transcribed as monocistronic transcripts (46). RNase E cleaves 8 nts upstream and 1–2 nts downstream of *hisR* and 4 nts upstream and 1–2 nts downstream of *cysT* (14). The majority of the higher molecular weight *hisR* tRNAs prior to Tris treatment converted to mature tRNA after the Tris treatment, suggesting a negligible amount of unprocessed tRNA in the wild type control at both the permissive and nonpermissive temperature (Figure 6A, lanes 1–2 and 9–10). In contrast, a significant amount of the high molecular weight *hisR* tRNA in the *rnpA49 ΔpcnB* double mutant was not converted to the size of mature tRNA after alkaline treatment (lanes 5–6 and 13–14) at both temperatures, which was consistent with their retaining the 8 nt 5′-leader sequence in the absence of RNase P. Furthermore, unlike *leuU* 5′-unprocessed tRNAs, alkaline treatment had no effect on these *hisR* 5′-unprocessed tRNAs, indicating that these were not aminoacylated.

Surprisingly, there was a dramatic reduction in the total amount of the *hisR* tRNA in the *rnpA49* single mutant, where bulk of the *hisR* tRNA retaining the 5′-leader sequence was missing at both temperatures (Figure 6A, lanes 3–4 and 11–12). Overexpression of *rnpB* restored *hisR* tRNA levels to almost wild type levels at the permissive temperature (Figure 6A, lanes 7–8), but not at the nonpermissive temperature (Figure 6A, lanes 15–16). The reduction in *hisR* tRNA species in the *rnpA49* and *rnpA49*/pAAK17 strains at 44°C was most likely due to polyadenylation dependent turnover of these species, since the absence of PAP I stabilized these species significantly in the *rnpA49 ΔpcnB* double mutant (Figure 6A, lanes 5–6, 13–14).

The level of *hisR* tRNA aminoacylation was only minimally reduced in all the *rnpA49* mutants at both the permissive and nonpermissive temperature [Figure 6C, PAT(P) and PAT(NP)]. The relative amount of chargeable tRNAs (RCT) was reduced significantly both at the permissive and nonpermissive temperature in the *rnpA49* single mutant compared to the wild type strain [Figure 6C, RCT(P) and RCT(NP)]. Under identical conditions, the chargeable tRNA (RCT) level was significantly higher in the *rnpA49 ΔpcnB* double mutant compared to the *rnpA49* single mutant. The percentage of aminoacylation in the *rnpA49*/pAAK17 mutant was higher than the *rnpA49* single mutant and similar to the wild type and *rnpA49 ΔpcnB* double mutant at the permissive temperature [PAT(P)], but similar to the *rnpA49* single mutant at the nonpermissive temperature [PAT(NP)]. Overexpression of *rnpB*, increased the amount of chargeable tRNAs available for aminoacylation in *rnpA49*/pAAK17 strain over ∼4-fold at the permissive temperature [RCT(P)], but failed to do so at the nonpermissive temperature [RCT(NP)].

The results obtained for *cysT, pheU* and *pheV* tRNAs were similar to what was observed with *hisR* except that the 5′ immature tRNAs seemed to be aminoacylated based on their reduction in size after alkaline treatment and their levels were not significantly reduced in the *rnpA49* mutant (data not shown). Furthermore, all these pre-tRNAs were destabilized in the *rnpA49* single mutant, but significantly stabilized in the *rnpA49 ΔpcnB* double mutant. In addition, M1 RNA overexpression in the *rnpA49*/pAAK17 strain led to improved aminoacylation levels of all tRNAs at the permissive temperature, but not at the nonpermissive temperature (data not shown).

5′-End maturation of tRNAs is not mandatory for aminoacylation.

The data presented above suggested that tRNAs with unprocessed 5′-ends were aminoacylated in the *rnpA49* mutant at the nonpermissive temperature (Figure 6A). In order to obtain additional support for this conclusion, we analyzed the proline tRNAs encoded by *proK, proL* and *proM*. Both *proK* and *proL* are monocistronic transcripts with 5′-leaders of 5–7 nt (23). *proM* is the last gene in a polycistronic transcript that is separated by RNase E cleavages at 4–7 nts up-

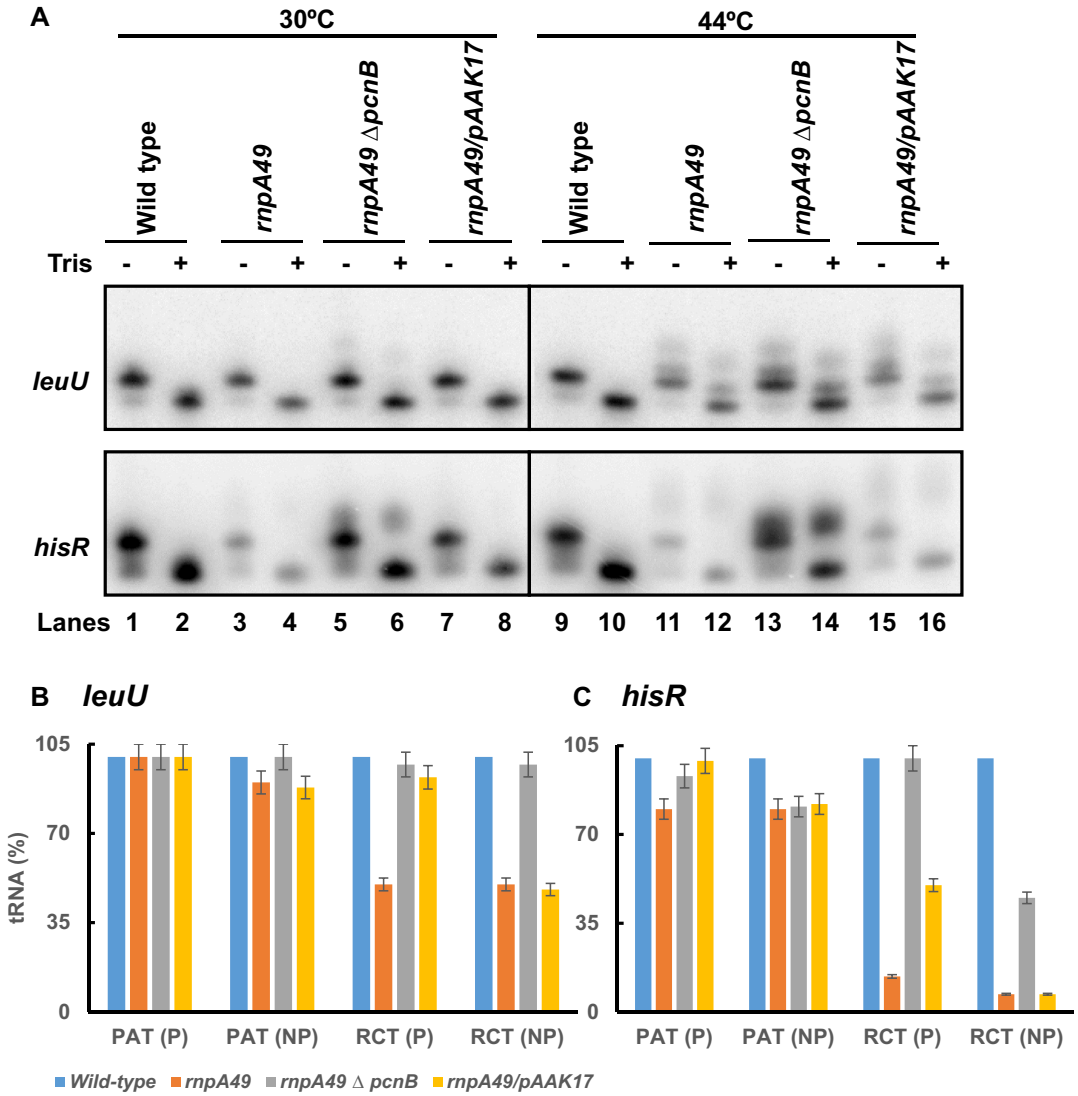

Figure 6. Analyses of $tRNA^{Leu2}$ (*leuU*) and $tRNA^{His}$ (*hisR*) aminoacylation by Northern blot analysis. (**A**) Total RNA isolated under acidic condition from various strains were either untreated (–) or treated (+) with 0.5 M Tris (pH 9) to chemically deacylate tRNAs and were separated using acid urea polyacrylamide gel (8%) as described in Materials and Methods. The blot was probed sequentially with a ^{32}P-end labeled oligonucleotide probes (LEUU-3′ and HISR-364, Supplementary Table S1) which hybridizes to *leuU* and *hisR* coding sequences. The percentage of aminoacylated tRNA (PAT) in each strain and the relative amount of chargeable tRNA (RCT) in each strain compared to the wild type strain at permissive (P) (30°C) and nonpermissive (NP) (44°C) temperature were calculated as described in the text. The PAT and RCT for *leuU* (**B**) and *hisR* (**C**) in various strains are average of at least three independent determinations. Multiple blots in each panel were run separately and merged at the vertical lines.

stream of the mature 5′-end (23,28). These tRNAs are matured at their 3′ termini by a one-step RNase E cleavage immediately downstream of the CCA determinant without the involvement of any 3′ → 5′ exonucleases (23). Accordingly, these tRNAs are not subject to polyadenylation, but are still dependent on RNase P for 5′-end maturation (23). Thus, most of the proline tRNAs were matured at the 3′ end, but remained immature at the 5′ end in an *rnpA49* mutant at the nonpermissive temperature (23). The RNA isolated at the permissive temperature showed that there was only one high molecular weight aminoacylated tRNA band which returned to the size of the mature tRNA after Tris treatment in all genetic backgrounds (Figure 7A, lanes 1–8). In contrast, the RNA isolated under nonpermissive conditions showed that there were two high molecular weight aminoacylated tRNA bands in all the *rnpA49* mutants (Figure 7A, lanes 11–16). After Tris treatment, both bands changed mobility with one still being larger than other. The smaller one was the fully matured tRNA identical to the wild type strain (lanes 9–10) and the larger one arose from the 5′-immature tRNA, which was observed only in the *rnpA49* mutants (lanes 11–16).

Furthermore, the percentage aminoacylation of proline tRNAs was experimentally identical in each strain at both the permissive and nonpermissive temperature (Figure 7B, PAT). There was a minor reduction in the amount of chargeable proline tRNAs in the *rnpA49* and *rnpA49*/pAAK17 strains, which was similar at both the permissive and nonpermissive temperature (Figure 7B, RCT). It has been shown that *metV, metW, metY* and *metZ* rep-

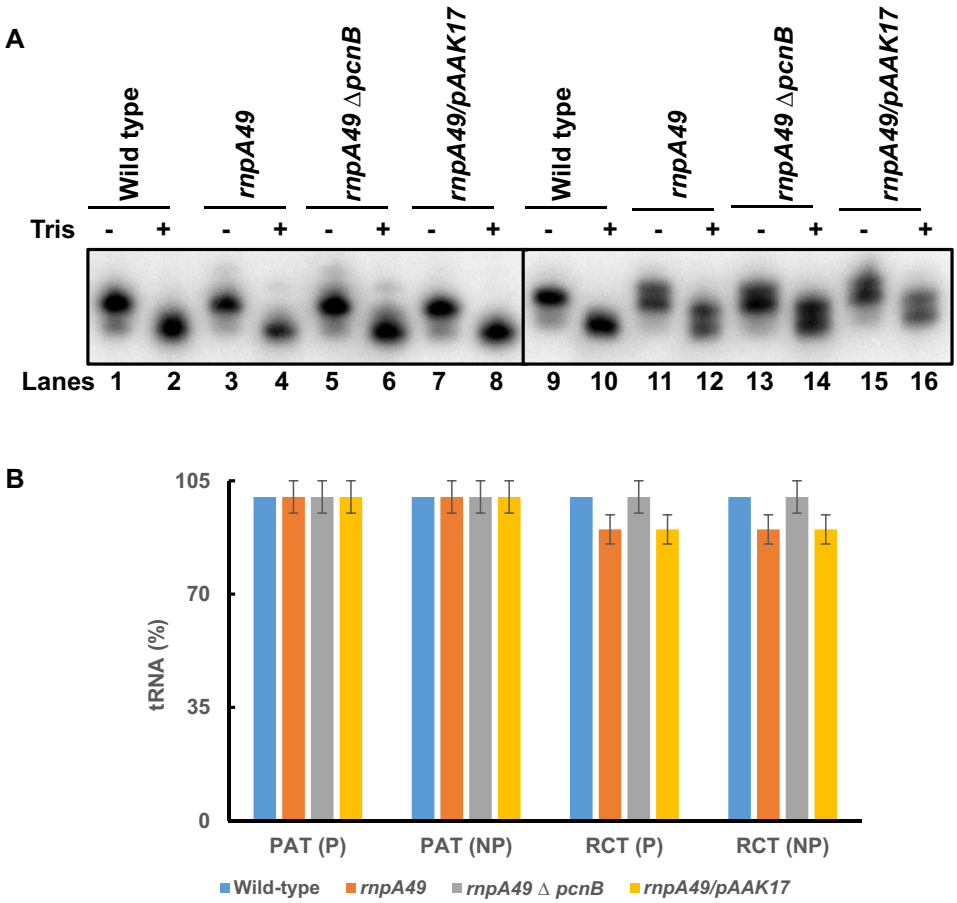

Figure 7. Analyses of $tRNA^{Pro}$ (*proK, proL* and *proM*) aminoacylation by Northern blot analysis. (**A**) Total RNA isolated under acidic condition was processed as described in Figure 6. The blot was probed with a ^{32}P-end labeled oligonucleotide probe (PROM, Supplementary Table S1) which hybridizes to the coding sequences of *proK, proL* and *proM*. (**B**) The PAT and RCT of *proM* in various strains at permissive (P) (30°C) and nonpermissive (NP) (44°C) temperature were calculated as described in the legends to Figure 6. The data presented in Figure 7B are average of at least three independent determinations. The RNA samples were run on two gels to accommodate all the samples and merged at the vertical line.

resenting the metf1 and metf2 isotypes are also not subject to polyadenylation (24) and are believed to be matured at the 3′-end by one-step RNase E cleavage (23). An aminoacylation analysis of these tRNAs yielded essentially similar results to *proK proL proM* (data not shown).

Pre-tRNAs with 5′-extension of < 8 nts and mature 3′ end are substrates for aminoacylation.

Subsequently, we analyzed the aminoacylation patterns of 35 tRNA transcripts encoding 17 tRNAs in various RNase P mutants in this study (Table 1). Only two of these tRNAs (Met m and Val2) were part of RNase P-dependent operons where no significant amount of 5′-unprocessed pre-tRNAs was detected in the *rnpA49* mutants. The rest of the tRNAs examined were processed mostly by initial endonucleolytic cleavages by enzymes other than by RNase P such that significant levels of 5′-unprocessed pre-tRNAs were detected in the *rnpA49* mutants. Based on the mobility of aminoacylated tRNAs in acid-urea gels, it was apparent that the pre-tRNAs with unprocessed 5′-ends ≥8 nts (*hisR, serV*) were not effectively aminoacylated with relative amount of chargeable tRNAs (RCT) <15% (Table 1). In contrast, the 12 pre-tRNAs with unprocessed 5′-end of <8 nts had much higher RCT levels, suggesting that they were effectively aminoacylated.

Inviability of *rnpA49* mutant is not due to lack of efficient *hisR* aminoacylation

Since $tRNA^{His}$ is unique in *E. coli,* is very unstable in the *rnpA49* mutant, and is not efficiently aminoacylated due to its longer unprocessed 5′-end (Figure 6A, C), it might be a possible candidate for causing the observed inviability. To answer this question, we overexpressed *hisR* from a plasmid (pBMK83) where *hisR* transcription was initiated at its mature 5′-end employing a *lac* promoter thereby avoiding the requirement of RNase P for 5′-end maturation. Northern analyses confirmed that there was ∼8 ± 1-fold increase in the mature tRNA level in *rnpA49*/pBMK83 strain compared to *rnpA49*/pBMK14 strain (Supplementary Figure S5). The relative chargeable tRNA (RCT) level of $tRNA^{His}$ in *rnpA49*/pBMK83 was even higher than the wild type strain (Table 1). However, no growth complementation in *rnpA49*/pBMK83 was observed at 44°C (data not shown), ruling out the lack of the mature *hisR* as the cause of the inviability in the *rnpA49* mutant.

Table 1. The leader lengths and the aminoacylation status of various tRNAs in the *rnpA49* mutant at nonpermissive temperatures

tRNAs	tRNA isotypes/operons	Leader length*	RCT** compared to the wild type strain (%)
Trp	*trpT*	3	80†
Phe	*pheU, pheV*	3–4	94 ± 5
Cys	*cysT*	4	30 ± 5
Ser1	*serT*	5	90†
Pro	*proK, proL, proM*	5–7	90 ± 5
Leu2	*leuU*	5–11[a]	50 ± 5
Asn	*asnT, asnU, asnV, asnW*	6–8	25†
Leu1	*leuT*	<8	32 ± 5
Leu3	*leuW*	<8	30†
Leu5	*leuX*	6–22[a]	90 ± 5
Lys	*lysQ, lysT, lysV, lysW, lysY, lysZ*	ND	20†
Met f2	*metY*	ND	67 ± 5
His	*hisR*	8	14 ± 3
His$^{\Psi}$	*hisR*$^{\Psi}$	0	110 ± 5
Ser3	*serV*	52	<15†
Met m	*metT, metU*	-[b]	<10
Val2	*valV valW*	-[b]	<10
Leu1	*leuQ leuP leuV*	-[b]	?
Met f1	*metZ metW metV*	-[b]	?

*Leader lengths are based on previous (14,23,27,46) and this study.
**Relative amount of chargeable tRNA (see text) in *rnpA49* mutant after one hour of growth at 44°C.
†Done once.
[a]5′ leader lengths are due to non-specific RNase E cleavage in the *rnpA49* mutant (14,22).
[b]RNase P dependent operons (13,14). No significant amounts of unprocessed pre-tRNAs were detected.
?: RCT could not be determined since these RNase P dependent tRNAs have RNase P independent tRNA isotypes.
ND: Not determined.
$^{\Psi}$tRNA^{His} expressed from pBMK83 (*hisR*$^{+}$/Cm^{R}).

DISCUSSION

Since it was first shown in 1972 that RNase P was required for the 5′-end maturation of tRNAs in *E. coli* (51), it has been thought that the processing of tRNA precursors must be perfect at both the 5′ and 3′ termini to permit aminoacylation. It was therefore assumed that 5′-end maturation was the essential function of the enzyme. However, here we have shown that 86% of the *E. coli* pre-tRNAs we tested (12 out of 14 pre-tRNAs) are aminoacylated between 20 and 94% of their wild type levels in the absence of RNase P, if their unprocessed 5′-extensions are <8 nts in length (Table 1). Only pre-tRNAs with 5′-extensions ≥8 nts appeared to be poor substrates for aminoacylation (Table 1).

The fact that the aminoacylation levels for the majority of the tRNAs were not reduced significantly in the absence of RNase P, under conditions where the pre-tRNAs were not matured at their 5′-ends (Figures 6, 7, Table 1, data not shown), strongly suggests that the tRNA aminoacylation machinery in *E. coli* has considerable tolerance for the presence of extra sequences of up to 7 nts at the 5′-ends of tRNA substrates. *In vivo* aminoacylation of 5′-extended tRNAs is consistent with the *in vitro* aminoacylation of a yeast tRNA^{Asp} with a 5′-extension (32) and the complementation of *E. coli* RNase P mutant with RNase P isozymes from *A. thaliana* (*At*RNase P), which cleave several *E. coli* pre-tRNAs in aberrant locations (36). Furthermore, it has also been shown that aminoacylation of a tRNA by its cognate aminoacyl-tRNA synthetase depends only on a limited number of nucleotides, primarily at the amino acid acceptor stem and the anticodon nucleotides (52,53). Taken together, the data presented here appear to rule out the loss of pre-tRNA aminoacylation in the *rnpA49* mutants as the primary reason for the strains' inviability at nonpermissive temperatures.

In contrast, our previous work has shown that at least seven polycistronic tRNA transcripts, encoding 25 tRNAs, in *E. coli* genome are absolutely dependent on initial RNase P processing to release pre-tRNAs that can be converted into aminoacylated species upon 3′-end maturation (13–15). When coupled with our recent finding using transcriptome analysis that three additional operons, encoding another 9 tRNAs, require initial RNase P processing (Mohanty and Kushner, manuscript in preparation), it is apparent that a significant drop in the steady-state levels of at least 34/86 tRNAs, including all seven valine species, will occur in the absence of RNase P. In fact, the data presented here shows a direct correlation between cessation of growth and a significant drop in the steady-state level of tRNAs, as low as ∼10% of wild type levels, derived from the *valV valW, secG leuU* and *leuQ leuP leuV* operons in the absence of RNase P (Figures 4, Supplementary Figures S3 and S4). Thus, the failure to generate pre-tRNAs from primary transcripts is the likely cause for the cessation of growth and loss of cell viability at nonpermissive temperatures.

This conclusion is supported by the results shown in Figure 4 and Supplementary Figures S3, S4 where the increased expression of the M1 RNA restored efficient processing of RNase P-dependent polycistronic operons coupled with a restoration of a wild type growth rate for the *rnpA49* mutant at the permissive temperature (Figure 3A). Since the RNase P holoenzyme containing the mutant protein has been shown *in vitro* to have a lower cleavage efficiency compared to the wild type holoenzyme at the permissive temperature (31), the increased expression of the M1 RNA (Figure 5) clearly helped restore the full catalytic activity of RNase P at 30°C (Figure 4, Supplementary Figures S3, S4).

While the protein subunit plays critical role in stabilizing the catalytically active conformation of M1 RNA (54) and helps define the substrate specificity of the RNase P enzyme (55), the defective C5 protein has reduced solubility at the nonpermissive temperature via a M1 RNA mediated quality control mechanism (56). Thus, although the overexpression of the M1 RNA was sufficient to improve RNase P activity at the permissive temperature, it failed to improve the processing of the RNase P-dependent primary tRNA transcripts (Figure 4 and Supplementary Figures S2-S3) at the nonpermissive temperature, resulting in the loss of complementation (Figure 3).

The inactivation of RNase P not only results in the failure of pre-tRNA generation from various RNase P-dependent operons (13–15), but it also leads to the accumulation of 5′-immature tRNAs derived from polycistronic operons processed by RNase E (28,30). While such pre-tRNAs undergo normal 3′-end maturation by one or more of the 3′ → 5′ exonucleases (RNase T, RNase PH, RNase D, RNase BN and RNase II), in competition with poly(A) polymerase I (PAP

I) (24), it was unexpected that many of the 5′-immature tRNAs showed increased levels of polyadenylation (Figures 1, 2, Supplementary Figure S1), resulting in ∼3-fold increase in short poly(A) tails (≤10 nt) (Figure 1). The absence of poly(A) tails in the *rnpA49 ΔpcnB* double mutant (Figures 1, 2 and Supplementary Figure S1), demonstrated that these tails were added by PAP I. It should also be noted that the significant differences observed in the percentage of immature 5′ and 3′-ends of tRNAs, polyadenylation levels, and extents of aminoacylation of various tRNAs are not entirely surprising, since the 86 tRNAs are matured through a very diverse set of processing pathways (57).

While aminoacylation of tRNAs requires a fully matured 3′-end terminated with the CCA trinucleotide, addition of a single nucleotide following the CCA determinant or alteration of the determinant by the removal of a nucleotide prevents aminoacylation (19). Increases in the chargeable tRNA levels in the *rnpA49 ΔpcnB* double mutant indicated that 5′-immature tRNAs were substrates for aminoacylation by tRNA synthetases (Figures 6 and 7). Surprisingly, despite similar processed fraction (PF) values for the *valV, valW* and *leuU* in the *rnpA49* and *rnpA49 ΔpcnB* mutants (Figure 4, Supplementary Figure S2), the relative chargeable tRNA (RCT) levels of these tRNAs were higher in the double mutant (Figure 6, data not shown), accounting for the growth differences at the permissive temperature.

Furthermore, polyadenylated pre-tRNAs not only are poor substrates for aminoacylation but are also degraded via poly(A)-dependent decay pathway (24,45). In fact, some pre-tRNAs such as *hisR* and *cysT* (Figure 6A, data not shown) seemed to be more susceptible to the poly(A)-dependent decay pathway, but were significantly stabilized in the *rnpA49 pcnB* double mutant. Consequently, the significant reduction of unique tRNAs, such as *hisR* and *cysT* (Figure 6A, data not shown) could be exacerbating inviability. However, overexpression of *hisR* (Supplementary Figure S5, Table 1) was not sufficient to restore the growth of *rnpA49* mutant at the nonpermissive temperature in this study (data not shown). Our earlier attempt to restore the growth of *rnpA49* mutant by complementing the expression of the seven valine tRNAs, independent of the RNase P processing requirement, was also not successful (15).

It appears that pre-tRNAs are increasingly polyadenylated in the *rnpA49* single mutant resulting in slower growth rate of the mutant (Figures 1, 2, Supplementary Figure S1). The continued growth of the *rnpA49 ΔpcnB* double mutant compared to the *rnpA49* single mutant at the nonpermissive temperature was consistent with the loss of polyadenylation in the double mutant facilitating increased stabilization of pre-tRNAs, which then could be aminoacylated. A significant improvement in the growth rate as well as in the aminoacylation of tRNAs in an *Δrnt rph-1 ΔpcnB* triple mutant has been previously observed (24). The significantly higher level of short poly(A) tails in the *Δrnt rph-1* double mutant (∼12-fold) compared to the *rnpA49* single mutant (∼3-fold) was consistent with increased levels of immature 3′-ends in the absence of RNase T and RNase PH compared to the absence of RNase P. The higher level of poly(A) tails in the *rnpA49 Δrnt rph-1* triple mutant (∼22-fold) compared to either of the mutants (Figure 1) suggested that failure to process at either the 5′- or 3′-end triggered independent tRNA polyadenylation events. Furthermore, the improvement in the 3′-end maturation of pre-tRNAs without any change in the 5′-end maturation in the *rnpA49 ΔpcnB* mutant (Figure 2B) indicated that the absence of PAP I facilitated the accessibility of tRNA 3′-ends by 3′→ 5′ exonucleases and that tRNA 3′-end maturation was not dependent on 5′-end maturation (Supplementary Figure S1). Faster 3′-end maturation of pre-tRNAs in the absence of PAP I has also been observed previously (24).

It is worth noting that the majority of tRNAs retaining 5′ extensions of ≤7 nts (27) in the absence of RNase P would be aminoacylated provided they have mature 3′-ends containing the CCA trinucleotides (Table 1). In addition, many pre-tRNAs retaining 5′-extensions ≥8 nts in the absence of RNase P quite often undergo non-specific endonucleolytic cleavages in their 5′ upstream regions, such as *leuU* (Figure 6A, Supplementary Figure S3), resulting in shorter 5′-extensions (14,22), making them substrates for aminoacylation. The exact reason why tRNAs with 5′ extensions ≥8 nts are poor substrates for aminoacylation is not clear at this time. It is possible that the longer 5′-extensions change the three-dimensional structure of the tRNA in such a way that it is no longer recognized by its cognate tRNA synthetase.

Since at least 34/86 tRNAs from 11 polycistronic tRNA operons are affected in the absence of RNase P, it is not likely that complementation of any single tRNA isotype will be sufficient to restore growth. Taken together, the data presented here show that it is not the failure of pre-tRNA aminoacylation, but rather the dramatic reduction in pre-tRNA levels derived from primary transcripts dependent on RNase P for their initial processing that is most likely responsible for the inviability of *rnpA49* mutants. Thus, the processing of polycistronic tRNA operons by RNase P should be considered its essential function. Furthermore, our data show that PAP I-dependent polyadenylation, which was once considered to be most relevant to mRNA metabolism in *E. coli,* also plays a more prominent role in tRNA metabolism.

SUPPLEMENTARY DATA

Supplementary Data are available at NAR Online.

FUNDING

National Institutes of Health (NIH) [GM57220, GM81544 to S.R.K.]. Funding for open access charge: NIH [GM81544].
Conflict of interest statement. None declared.

REFERENCES

1. Condon,C. and Putzer,H. (2002) The phylogenetic distribution of bacterial ribonucleases. *Nucleic Acids Res.*, **30**, 5339–5346.
2. Altman,S. (1989) Ribonuclease P: an enzyme with a catalytic RNA subunit. *Adv. Enzymol. Relat. Areas Mol. Biol.*, **62**, 1–36.
3. Gopalan,V., Vioque,A. and Altman,S. (2002) RNase P: variations and uses. *J. Biol. Chem.*, **277**, 6759–6762.
4. Randau,L., Schroder,I. and Soll,D. (2008) Life without RNase P. *Nature*, **453**, 120–123.

5. Hall,T.A. and Brown,J.W. (2001) The ribonuclease P family. *Methods Enzymol.*, **341**, 56–77.
6. Lai,L.B., Vioque,A., Kirsebom,L.A. and Gopalan,V. (2010) Unexpected diversity of RNase P, an ancient tRNA processing enzyme: challenges and prospects. *FEBS Lett.*, **584**, 287–296.
7. Gobert,A., Gutmann,B., Taschner,A., Gossringer,M., Holzmann,J., Hartmann,R.K., Rossmanith,W. and Giege,P. (2010) A single *Arabidopsis* organellar protein has RNase P activity. *Nat. Struct. Mol. Biol.*, **17**, 740–744.
8. Holzmann,J. and Rossmanith,W. (2009) tRNA recognition, processing, and disease: hypotheses around an unorthodox type of RNase P in human mitochondria. *Mitochondrion*, **9**, 284–288.
9. Holzmann,J., Frank,P., Loffler,E., Bennett,K.L., Gerner,C. and Rossmanith,W. (2008) RNase P without RNA: identification and functional reconstitution of the human mitochondrial tRNA processing enzyme. *Cell*, **135**, 462–474.
10. Rossmanith,W. and Holzmann,J. (2009) Processing mitochondrial (t)RNAs: new enzyme, old job. *Cell Cycle*, **8**, 1650–1653.
11. Taschner,A., Weber,C., Buzet,A., Hartmann,R.K., Hartig,A. and Rossmanith,W. (2012) Nuclear RNase P of *Trypanosoma brucei*: a single protein in place of the multicomponent RNA-protein complex. *Cell Rep.*, **2**, 19–25.
12. Blattner,F.R., Plunkett,G. III, Bloch,C.A., Perna,N.T., Burland,V., Riley,M., Collado-Vides,J., Glasner,J.D., Rode,C.K., Mayhew,G.F. *et al.* (1997) The complete sequence of *Escherichia coli* K-12. *Science*, **277**, 1453–1474.
13. Mohanty,B.K. and Kushner,S.R. (2007) Ribonuclease P processes polycistronic tRNA transcripts in *Escherichia coli* independent of ribonuclease E. *Nucleic Acids Res.*, **35**, 7614–7625.
14. Mohanty,B.K. and Kushner,S.R. (2008) Rho-independent transcription terminators inhibit RNase P processing of the *secG leuU* and *metT* tRNA polycistronic transcripts in *Escherichia coli*. *Nucleic Acids Res.*, **36**, 364–375.
15. Agrawal,A., Mohanty,B.K. and Kushner,S.R. (2014) Processing of the seven valine tRNAs in *Escherichia coli* involves novel features of RNase P. *Nucleic Acids Res.*, **42**, 11166–11179.
16. Alifano,P., Rivellini,F., Piscitelli,C., Arraiano,C.M., Bruni,C.B. and Carlomagno,M.S. (1994) Ribonuclease E provides substrates for ribonuclease P-dependent processing of a polycistronic mRNA. *Genes & Develop.*, **8**, 3021–3031.
17. Li,Y. and Altman,S. (2003) A specific endoribonuclease, RNase P, affects gene expression of polycistronic operon mRNAs. *Proc. Natl. Acad. Sci. USA*, **100**, 13213–13218.
18. Li,Y., Cole,K. and Altman,S. (2003) The effect of a single, temperature-sensitive mutation on global gene expression in *Escherichia coli*. *RNA*, **9**, 518–532.
19. Reuven,N.B. and Deutscher,M.P. (1993) Substitution of the 3′ terminal adenosine residue of transfer RNA *in vivo*. *Proc. Natl. Acad. Sci. U.S.A.*, **90**, 4350–4353.
20. Li,Z. and Deutscher,M.P. (1994) The role of individual exoribonucleases in processing at the 3′ end of *Escherichia coli* tRNA precursors. *J. Biol. Chem.*, **269**, 6064–6071.
21. Li,Z., Pandit,S. and Deutscher,M.P. (1998) 3′ exoribonucleolytic trimming is a common feature of the maturation of small, stable RNAs in *Escherichia coli*. *Proc. Natl. Acad. Sci. U.S.A.*, **95**, 2856–2861.
22. Mohanty,B.K. and Kushner,S.R. (2010) Processing of the *Escherichia coli leuX* tRNA transcript, encoding $tRNA^{leu5}$, requires either the 3′-5′ exoribonuclease polynucleotide phosphorylase or RNase P to remove the Rho-independent transcription terminator. *Nucleic Acids Res.*, **38**, 597–607.
23. Mohanty,B.K., Petree,J.R. and Kushner,S.R. (2016) Endonucleolytic cleavages by RNase E generate the mature 3′ termini of the three proline tRNAs in *Escherichia coli*. *Nucleic Acids Res.*, **44**, 6350–6362.
24. Mohanty,B.K., Maples,V.F. and Kushner,S.R. (2012) Polyadenylation helps regulate functional tRNA levels in *Escherichia coli*. *Nucleic Acids Res.*, **40**, 4589–4603.
25. Schedl,P. and Primakoff,P. (1973) Mutants of *Escherichia coli* thermosensitive for the synthesis of transfer RNA. *Proc. Natl. Acad. Sci. USA*, **70**, 2091–2095.
26. Kirsebom,L.A., Baer,M.F. and Altman,S. (1988) Differential effects of mutations in the protein and RNA moieties of RNase P on the efficiency of suppression by various tRNA suppressors. *J. Mol. Biol.*, **204**, 879–888.
27. Fredrik Pettersson,B.M., Ardell,D.H. and Kirsebom,L.A. (2005) The length of the 5′ leader of *Escherichia coli* tRNA precursors influences bacterial growth. *J. Mol. Biol.*, **351**, 9–15.
28. Li,Z. and Deutscher,M.P. (2002) RNase E plays an essential role in the maturation of *Escherichia coli* tRNA precursors. *RNA*, **8**, 97–109.
29. Li,Z., Gong,X., Joshi,V.H. and Li,M. (2005) Co-evolution of tRNA 3′ trailer sequences with 3′ processing enzymes in bacteria. *RNA*, **11**, 567–577.
30. Ow,M.C. and Kushner,S.R. (2002) Initiation of tRNA maturation by RNase E is essential for cell viability in *E. coli. Genes Dev.*, **16**, 1102–1115.
31. Baer,M.F., Wesolowski,D. and Altman,S. (1989) Characterization *in vitro* of the defect in a temperature-sensitive mutant of the protein subunit of RNase P from *Escherichia coli*. *J Bacteriol.*, **171**, 6862–6866.
32. Perret,V., Florentz,C. and Giege,R. (1990) Efficient aminoacylation of a yeast transfer RNA^{Asp} transcript with a 5′ extension. *FEBS Lett.*, **270**, 4–8.
33. Burkard,U., Willis,I. and Soll,D. (1988) Processing of histidine transfer RNA precursors. Abnormal cleavage site for RNase P. *J. Biol. Chem.*, **263**, 2447–2451.
34. Connolly,S.A., Rosen,A.E., Musier-Forsyth,K. and Francklyn,C.S. (2004) G-1:C73 recognition by an arginine cluster in the active site of *Escherichia coli* histidyl-tRNA synthetase. *Biochemistry*, **43**, 962–969.
35. Tamaki,S., Tomita,M., Suzuki,H. and Kanai,A. (2018) Systematic analysis of the binding surfaces between tRNAs and their respective aminoacyl tRNA synthetase based on structural and evolutionary data. *Front. Genet.*, **8**, 227.
36. Gossringer,M., Lechner,M., Brillante,N., Weber,C., Rossmanith,W. and Hartmann,R.K. (2017) Protein-only RNase P function in *Escherichia coli*: viability, processing defects and differences between PRORP isoenzymes. *Nucleic Acids Res.*, **45**, 7441–7454.
37. Jain,S.K., Gurevitz,M. and Apirion,D. (1982) A small RNA that complements mutants in the RNA processing enzyme ribonuclease P. *J. Mo.l Biol.*, **162**, 515–533.
38. Jensen,K.G. (1993) The *Escherichia coli* K-12 "wild types" W3110 and MG1655 have an *rph* frameshift mutation that leads to pyrimidine starvation due to low *pyrE* expression levels. *J. Bacteriol.*, **175**, 3401–3407.
39. O'Hara,E.B., Chekanova,J.A., Ingle,C.A., Kushner,Z.R., Peters,E. and Kushner,S.R. (1995) Polyadenylylation helps regulate mRNA decay in *Escherichia coli*. *Proc. Natl. Acad. Sci. U.S.A.*, **92**, 1807–1811.
40. Mohanty,B.K. and Kushner,S.R. (1999) Analysis of the function of *Escherichia coli* poly(A) polymerase I in RNA metabolism. *Mol. Microbiol.*, **34**, 1094–1108.
41. Mohanty,B.K. and Kushner,S.R. (2019) Analysis of post-transcriptional RNA metabolism in prokaryotes. *Methods*, **155**, 124–130.
42. Mohanty,B.K. and Kushner,S.R. (2014) *In vivo* analysis of polyadenylation in prokaryotes. *Methods Mol Biol.*, **1125**, 229–249.
43. Mohanty,B.K., Giladi,H., Maples,V.F. and Kushner,S.R. (2008) Analysis of RNA decay, processing, and polyadenylation in *Escherichia coli* and other prokaryotes. *Methods Enzymol.*, **447**, 3–29.
44. Wang,R.F. and Kushner,S.R. (1991) Construction of versatile low-copy-number vectors for cloning, sequencing and gene expression in *Escherichia coli*. *Gene*, **100**, 195–199.
45. Mohanty,B.K. and Kushner,S.R. (2013) Deregulation of poly(A) polymerase I in *Escherichia coli* inhibits protein synthesis and leads to cell death. *Nucleic Acids Res.*, **41**, 1757–1766.
46. Bowden,K.E., Wiese,N.S., Perwez,T., Mohanty,B.K. and Kushner,S.R. (2017) The *rph-1*-encoded truncated RNase PH protein inhibits RNase P maturation of pre-tRNAs with short leader sequences in the absence of RppH. *J. Bacteriol.*,**199**, doi:10.1128/JB.00301-17.
47. Baer,M.F., Reilly,R.M., McCorkle,G.M., Hai,T.Y., Altman,S. and RajBhandary,U.L. (1988) The recognition by RNase P of precursor tRNAs. *J. Biol. Chem.*, **263**, 2344–2351.
48. Motamedi,H., Lee,K., Nichols,L. and Schmidt,F.J. (1982) An RNA species involved in *Escherichia coli* ribonuclease P activity. Gene cloning and effect on transfer RNA synthesis *in vivo*. *J. Mol. Biol.*, **162**, 535–550.
49. Guerrier-Takada,C., Gardiner,K., Marsh,T., Pace,N. and Altman,S. (1983) The RNA moiety of ribonuclease P is the catalytic subunit of the enzyme. *Cell*, **35**, 849–857.

50. Kim,Y. and Lee,Y. (2009) Novel function of C5 protein as a metabolic stabilizer of M1 RNA. *FEBS Lett.*, **583**, 419–429.
51. Robertson,H.D., Altman,S. and Smith,J.D. (1972) Purification and properties of a specific *Escherichia coli* ribonuclease which cleaves a tyrosine transfer ribonucleic acid presursor. *J. Biol. Chem.*, **247**, 5243–5251.
52. Naganuma,M., Sekine,S., Chong,Y.E., Guo,M., Yang,X.L., Gamper,H., Hou,Y.M., Schimmel,P. and Yokoyama,S. (2014) The selective tRNA aminoacylation mechanism based on a single G*U pair. *Nature*, **510**, 507–511.
53. Beuning,P.J. and Musier-Forsyth,K. (1999) Transfer RNA recognition by aminoacyl-tRNA synthetases. *Biopolymers*, **52**, 1–28.
54. Buck,A.H., Dalby,A.B., Poole,A.W., Kazantsev,A.V. and Pace,N.R. (2005) Protein activation of a ribozyme: the role of bacterial RNase P protein. *EMBO J.*, **24**, 3360–3368.
55. Sun,L., Campbell,F.E., Zahler,N.H. and Harris,M.E. (2006) Evidence that substrate-specific effects of C5 protein lead to uniformity in binding and catalysis by RNase P. *EMBO J.*, **25**, 3998–4007.
56. Son,A., Choi,S.I., Hon,G. and Seong,B.L. (2015) M1 RNA is important for the in-cell solubility of its cognate C5 protein: implications for RNA-mediated protein folding. *RNA Biol.*, **12**, 1198–1208.
57. Mohanty,B.K. and Kushner,S.R. (2019) New insights into the relationship between tRNA processing and polyadenylation in *Escherichia coli*. *Trends Genet.*, **35**, 434–445.